Journal of the Korean Magnetic Resonance Society **1997**, *1*, 79-94

Solution Structure of Bovine Pancreatic Trypsin Inhibitor using NMR Chemical Shift Restraints

Kyunglae Park and Wilfred F. van Gunsteren†

College of Pharmacy, Chungnam National University,
Daejeon 305-764, Korea
†Physical Chemistry, ETH Zentrum, CH-8092 Zürich, Switzerland
Received October 24, 1997

Abstract: The solution structure of bovine pancreatic trypsin inhibitor(BPTI) has been refined by NMR chemical shift data of $C_\alpha H$ using classical molecular dynamics simulation. The structure dependent part of the observable chemical shift was modeled by ring current effect, magnetic anisotropy effect from the nearby groups, whereas the structure independent part was replaced with the random coil shift. A new harmonic function derived from the differences between the observed and calculated chemical shifts was added into physical force field as an pseudo potential energy term with force constant of 250 $kJmol^{-1}ppm^{-2}$. During the 1.5 ns molecular dynamics simulation with chemical shift restraints BPTI has accessed different conformation space compared to crystal and NOE driven structure.

INTRODUCTION

Since the NMR techniques are available for biomolecular system the number of solution structures of protein reported yearly in the protein data bank are also steadily increasing. Most of them are the results of the intensive computational study utilizing the NOE and J coupling data measured in solution state. Although the methodology is nowadays a standardized one, in order to construct a solution structure from NOE distance data alone a sufficient number of NOE

signals should be detected and analyzed. The consequence of the lack of NOE data is that the NMR structures reported in the literature have often irregular resolution and the degree of conformational freedom is high relative to the crystal structure. Prior to these derived data, fortunately, NMR experiments yield the primary observable, the chemical shift of each resonance, which has no interpretational ambiguity in the measurement and contains uniform information about the conformation or the secondary structure. Generally the conformation dependent part of the experimental chemical shift can be approximated as the sum of ring current effects from Phenylalnine, Tyrosine, Tryptophane and Histidine, magnetic anisotropy effects from C = O and (O =)C − N bonds of peptides.

The potential power of chemical shift as an additional information source has long been recognized and there has been also continuous efforts to improve the calculation algorithm[1] and to optimize the structural parameters[2] in order to better correlate the predicted to the observed chemical shifts. In the literature a number of structural studies were also reported[3,4] in conjunction with molecular dynamics(MD) simulation including chemical shift data but the expected improvement in the precision of the structure could not be verified.

Recently our group has reassessed this problem and developed the methodological details of chemical shift restraining(CSR)[5] MD consistent with the conventional MD framework and the stability was tested successfully. Using this new method with chemical shift restraints the solution structure of bovine pancreatic trypsin inhibitor(BPTI) was reinvestigated in the present work. BPTI is a small protein(58 residues) with very high stability and therefore suitable for test of new experimental and theoretical methods. Crystal structures from X-ray and neutron diffraction methods have been determined and reported[6]. Starting with the first determination of solution structure of BPTI by means of NMR data alone[7] there are many studies in the literature concerning the structural and dynamic properties of this protein in solution state.

In the present work we have performed 1.5ns MD simulations with and without chemical shift restraints. The CSR MD yielded a new set of structures which satisfies the measured chemical shift data. The comparison of these structures with X-ray structure and conventional NOE driven structure will demonstrate the usefulness and complementarity of chemical shift values for further refinement of the solution structures in general. In addition the structural change of BPTI was analyzed to trace the behavior of the protein with respect to backbone and side chain conformation during the whole simulation time window.

METHODS

The experimental chemical shift, δ_{exp} of nucleus of a structured protein can be expressed in terms of local and non-local parts according to their origin and property of the contributions. The local term mainly arising from diamagnetic and paramagnetic shielding around the nucleus was assumed to be independent of the secondary structure. We can replace this term by the random coil shift[8], $\delta_{\text{random coil}}$, which was experimentally measured using unstructured tetrapeptides. The non-local term can then be assigned to secondary shift, δ_{sec}, which may include approximately ring current effects from nearby aromatic side chains and magnetic anisotropy effects of peptides from spatial vicinity. The secondary shift can thus be described as,

$$\delta_{sec} = \delta_{exp} - \delta_{\text{random coil}} \quad [1]$$

In our previous work[5] the theoretical secondary shift, δ_{cal} was accordingly represented as the sum of ring current term, δ_{rc}, and magnetic anisotropy term, δ_{ma}, which were modeled by the classical method from Johnson and Bovey[9] and ApSimon *et al.*[10], respectively.

$$\delta_{cal} = \delta_{rc} + \delta_{ma} \quad [2]$$

The difference between the observation, δ_{sec}, and the prediction, δ_{cal}, was the basis for the harmonic potential,

$$V_{cs} = \frac{1}{2} K_{cs} (\delta_{cal} - \delta_{sec})^2 \quad [3]$$

where K_{cs} is the restraining force constant defined in $\text{kJmol}^{-1}\text{ppm}^{-2}$. The special version[5] of GROMOS96 modeling package program[11] was used to restrain the atomic position with respect to the input chemical shift data.

The simulations were perfomed using vacuum force field of GROMOS96[11] including chemical shift potential of Eq. 3. The parameters used in the simulations and equilibriation steps are summarized in Table 1. As a starting structure we used 1BPI[12] of crystal form II from Brookhaven Data Bank and the chemical shift values were those reported by Wagner *et al.*[13] To incorporate the measurement condition at pH=4.6 and 309K we used charged forms for Arg, Lys, Glu and Asp and simulation temperature of 309K. There were 10 protonated and 4 deprotonated residues and the net charge of BPTI molecule was $+6e$. Nonpolar

hydrogens were treated as united atoms and polar and aromatic hydrogen atoms were treated explicitly, which resulted in a total of 604 protein atoms. All bond lengths were kept fixed during the simulations with the SHAKE procedure[14]. For nonbonded interactions we used a twin range method[15]. The electrostatic interactions within cutoff range between 8 and 14 Å were only calculated every 10 time steps of 2 fs each, when the pair list was updated.

The BPTI was equilibriated in several steps. In the first stage we performed a position restraining energy minimization on the protein atoms with steepest descent method. As a reference structure we used the starting structure

Table 1. Simulation parameters and steps

force field	43B1 + chemical shift force	
starting structure	1BPI	
protein atoms	604	
short - long range cutoff (Å)	8 - 14	
pair list update (fs)	20	
simulation time step (fs)	2	
energy minimization[a] with position restraining	68 steps	
K_{pr}(kJmol^{-1}Å^{-2})	90	
MD time(ps) with position restraining	2	
K_{pr}	9	
initial bath temperature(K)	100	
temperature coupling relaxation time (ps)	0.01	
MD time(ps) with position restraining	2	
K_{pr}	0.9	
bath temperature(K)	200	
MD time(ps)	3	
bath temperature(K)	309	
temperature coupling relaxation time (ps)	0.1	
simulation	**A**	**B**
MD time(ps) with chemical shift restraining	3	3
K_{cs}(kJmol^{-1}ppm^{-2})	0	250
Long time(ps) MD simulation	1500	1500
K_{cs}	0	250
sampling frequency(ps) for trajectories	0.1	0.1

and the force constant for the position restraining harmonic potential was kept 90 $kJmol^{-1}Å^{-2}$ during 68 steps of minimization. The relaxation of the possible strain in crystal structure was done by molecular dynamics method with decreasing position restraining force constant and with increasing bath temperature. In all simulations, the temperatures of the solute was coupled to a temperature bath. In the first 2 ps MD calculation the position restraining force constant was reduced to 9 $kJmol^{-1}Å^{-2}$ and the initial atomic velocities were taken from a Maxwell-Boltzmann distribution at 100 K. The temperature coupling relaxation time to the temperature and pressure bath were set to 0.01ps. For the next 2 ps MD the force constant K_{pr} was reduced further to 0.9 $kJmol^{-1}Å^{-2}$ and the bath temperature was increased to 200 K. From the third step (3 ps), we applied no position restraining and raised the bath temperature to 309 K and the temperature coupling time to 0.1ps.

From the final 3ps of equilibriation on we carried out two different simulations. In simulation **A** we continued the third stage without any restraining. Simulation **B** were run using chemical shift restraining with force constants of 250 $kJmol^{-1}ppm^{-2}$, which corresponds to the relative tolerance of chemical shift deviations of about 0.1 ppm. The starting structures for these stages were taken from the final coordinates of the third equilibriation stage. All chemical shifts of non-glycine $C_\alpha H$ except first and last residues are restrained in the simulation **B** and the long range cutoff of 14 Å was also used to determine groups contributing to the chemical shift value for a given nucleus. After the fourth steps the time origin was reset to zero and the three simulations were run for 1.5ns with the same parameters of the final steps. Coordinates of the solution after every 10 ps were saved to disk and to generate the trajectories the coordinates were sampled every 0.1 ps.

RESULTS AND DISCUSSIONS

For the analysis of the simulation results the internal coordinates of protein atoms were averaged over every 10ps MD trajectory. The first sign of change in overall structure can be seen in the total positional deviation of the protein atoms from the starting structure, as shown in Fig. 1. In both of the simulations the atomic positions deviate from the first MD stage on and converges to about 2.5Å for C_α atoms(Fig. 1a) and about 3.5Å for all atoms(Fig. 1b) after 500ps of simulations. After about 1ns, however, the deviation is slightly increasing again,

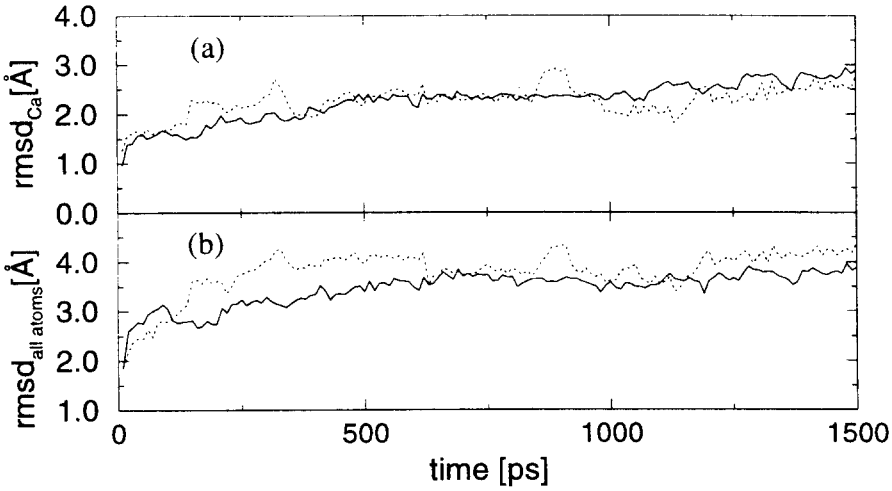

Fig. 1. Root mean square deviation of Ca atoms(a) and all atoms(b) from the starting structure during the simulation without(dotted) and with(solid) chemical shift restraints averaged over every 10 ps windows.

which means that the molecular system is still moving to some other conformation space and thus the simulation time of 1.5ns is obviously not enough to get into the final equilibrated space.

To visualize the details of these deviations the distance difference maps are shown in Fig. 2, where the average structures of final 10ps of simulations were compared to the starting structure. Here the distance of Ca atom of ith residue to that of jth residue of the simulated structure was subtracted from that of the starting structure and this double distance values were represented with respect to ith and jth residue numbers. Here the starting structure was equilibrated with position restraining MD and we found that this structure had almost the same conformation with the original structure 1BPI[12] from protein data bank. This results of analysis reveals a different aspect of the MD simulation from that of the positional fluctuations in Fig. 1. Although the values of total atomic deviations are almost identical for free(**A**) and chemical shift restrained(**B**), but the position of this deviation reveals quite different behaviors. In case of free MD(**A**) the change has concentrated on the distance of 12-13th and 38-40th residues to 45-54th residues(Fig. 2a). A similar results were also reported in a MD study by Brunne *et al.*[16], where the largest flexibility and deviation from crystal and NMR structure were found at 12-16th 36-38th residues in free simulation. With

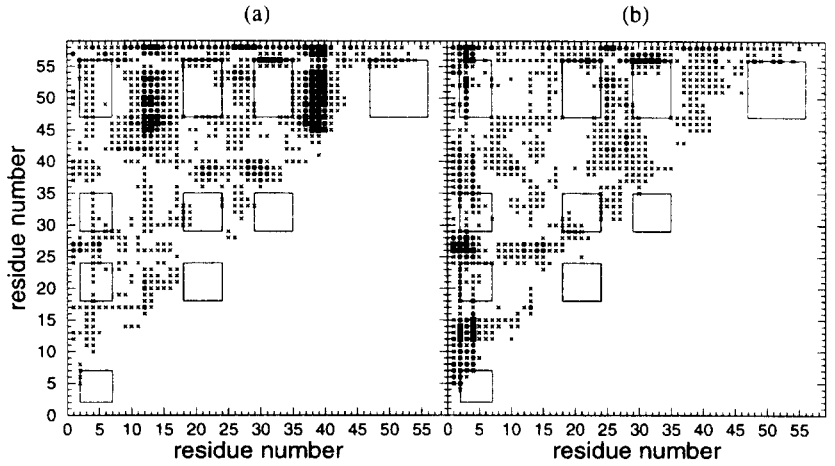

Fig. 2. Distance difference map of the final structure from simulation without(a) and with(b) chemical shift restraints with respect to the starting structure. The distance difference was marked with × for 1.0 - 3.0Å , filled circle for 3.0 - 5.0Å and filled square above 5.0Å .

the chemical shift restraints(simulation **B**), on the other hand, we found that the positional change occurred mainly on the first and last ends of the protein(Fig. 2b). In both of the two simulations the change has occurred in the coiled peptide regions, while the α helix and β sheet structure were conserved during the molecular dynamics. Although not presented here we have found furthermore that there is no significant differences in the Ca positions between the final restrained structure from simulation **B**, x-ray and NMR structures. Therefore the change during the chemical shift restraining must have occurred in the backbone dihedral angles and/or in the side chain conformations.

The overall size of the protein molecule, as given with the radius of gyration in Fig. 3, shows a more significant difference of the two simulations. The well known fact that the vacuum simulation may be generally accompanied by a contraction of the structure can be also seen here in free simulation **A**, but in the chemical shift restrained simulation **B** the size of the molecule retains almost the level of the starting structure during the whole time window. From this observation we can conclude that this general drawback of vacuum force field in the absence of solvent molecules is obviously overcome by the use of additional chemical shift restraints for the reasonable prediction of solution structure.

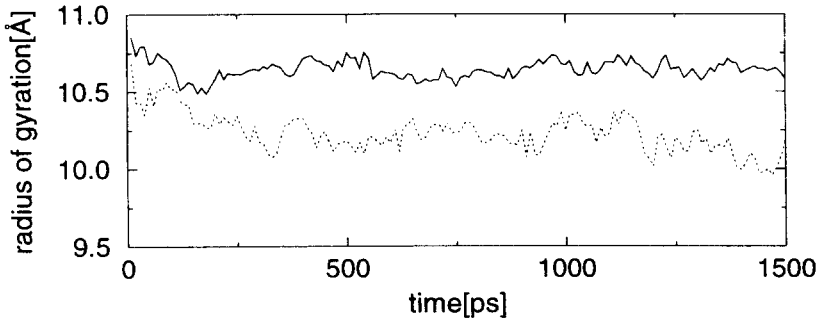

Fig. 3. The dimension of molecule expressed by radius of gyration during the simulation for free(dotted) and restrained(solid) MD.

The mobility of protein can then be represented by root mean square fluctuation (rmsf) of all atoms and Ca atoms versus time axis in Fig. 4. The total flexibility of the backbone chain, as shown in Fig. 4a, is basically identical for simulation **A** and **B**, while the side chain mobility, represented by total rmsf of all atoms in Fig. 4b, is slightly higher in unrestrained simulation **A** than in the chemical shift restrained simulation **B**. This explains clearly that the chemical shift values reduce the size of conformation space the side chain of the protein molecule can visit.

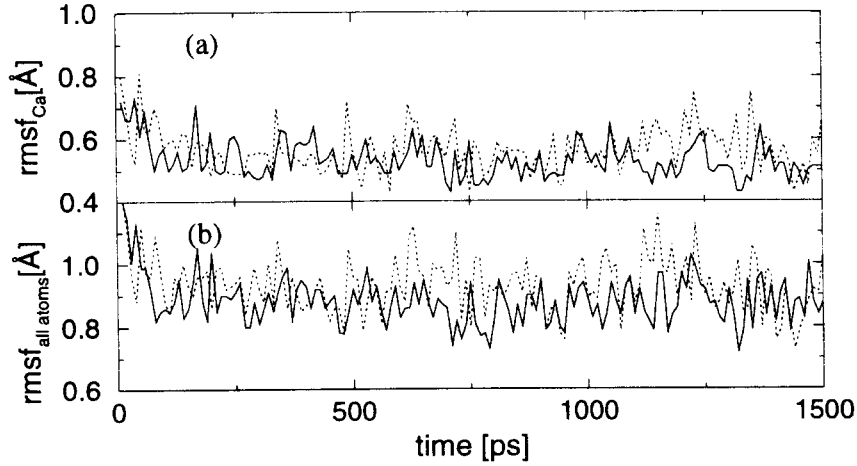

Fig. 4. Root mean square fluctuation of Ca atoms(a) and all atoms(b) during the simulation without(dotted) and with(solid) chemical shift restraints averaged over every 10 ps windows.

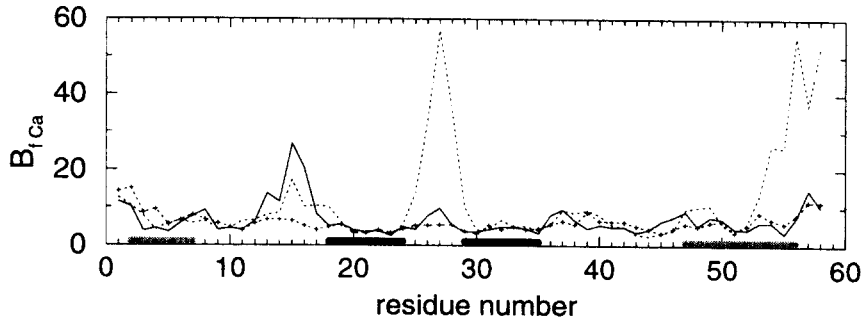

Fig. 5. The flexibility of Ca atoms with respect to residue number without(dotted) and with(solid) chemical shift restraints calculated using Eq. 2 from atomic fluctuation. The values were averaged from the final 10 ps trajectories and the B-factor of the crystal structure 1BPI(+) was given for comparison and the gray and black band on the x-axis denote the position of helical and strand conformation.

If one analyzes the atomic positional fluctuation with respect to each amino acid residue, averaged from the last 10ps time trajectory of the simulation, we can observe a detailed picture of the mobility of the protein, as shown in Fig. 5.. For reasons of better comparison with the crystal structure we converted the rmsf(Δr) of Ca atoms of each residue to crystallographic B-factor using Eq. 4:

$$B = (8\pi^2/3)\Delta r^2 \qquad [4]$$

The real meaning of B-factor reported from crystal structure is certainly different from that of the MD simulation. The crystallographic B-factor informs about the resolution or precision of corresponding atomic position, whilst the MD simulation B-factor gives information about the flexibility or mobility of atoms during the simulation time window. The comparison, therefore, should be interpreted only in a qualitative way instead of the absolute value itself. We then have taken Δr averaged from the last 10ps time trajectory of the simulation and shown in Fig. 4, which revealed regional difference in the protein backbone chain. As in the deviation of the atomic positions a similar behaviors were found here as shown in Fig. 5. The greater mobility can be observed in the coiled regions, while the structured part(residues 2-7, 18-24, 29-35 and 47-56) of the protein reaches almost the rigidity of the crystal structure as described by B-factors of x-ray structure for comparison. The chemical shift restraints(**B**) can also reduce the degree of mobility compared to the case of free MD(**A**).

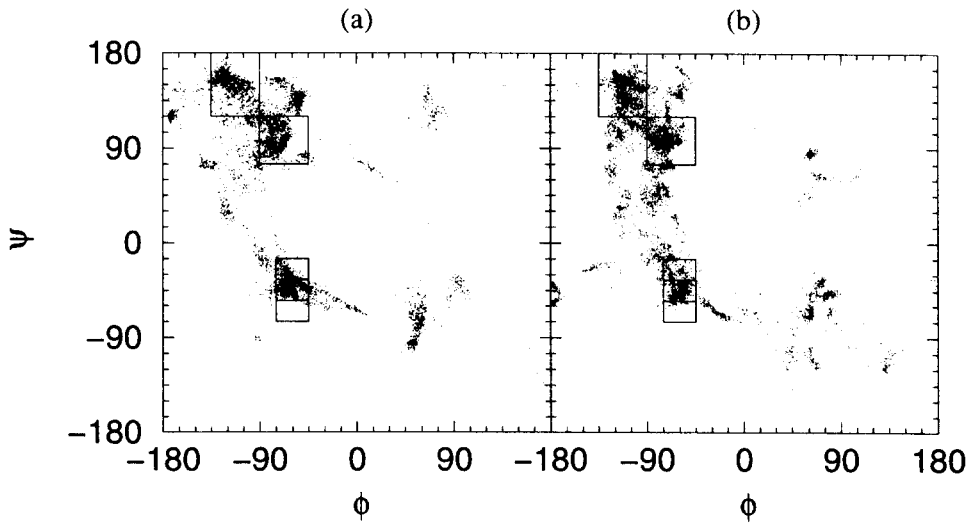

Fig. 6. The backbone conformation space visited by the protein during the free(a) and restrained(b) MD simulation. The squared parts from top to down correspond parallel, antiparallel β-, 3_{10}-, α- and π-helical regions.

The whole time course of the simulation was also analyzed with respect to the backbone dihedral angles of each residue. In Fig. 6 the conformation described by ϕ and ψ angles of were plotted in Ramachandran diagram to show the dynamic behavior during 1.5ns of simulation time. Here the parallel and antiparallel β-sheet components can be assigned if the dihedral angle lies in the range from -90° to -45° and from -135° to -90° for ϕ and from 75° to 120° and from 120° to 180° for ψ, respectively. For 3_{10}-, α- and π-helical conformation the range

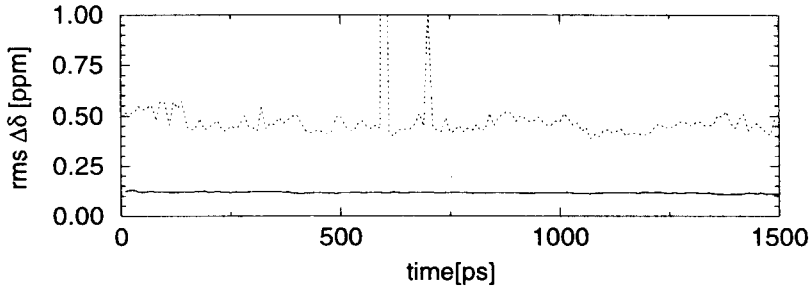

Fig. 7. Root mean square deviation of chemical shift δ_{cal} from δ_{sec} during the simulation without(dotted) and with(solid) chemical shift restraints averaged over every 10 ps windows.

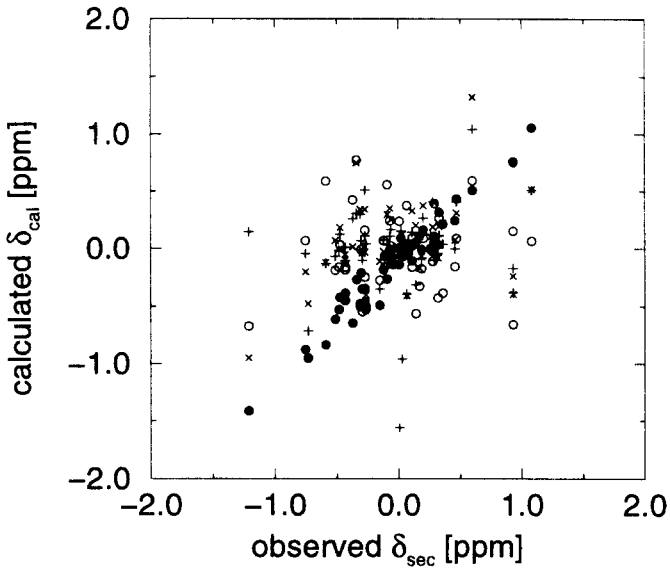

Fig. 8. Correlation diagram of chemical shifts from the final structures of simulation without(○) and with(●) chemical shift restraints. For comparison the values calculated from the x-ray crystal structure(×) and NMR structure(+) are also shown.

from -75° to -45° for ϕ and from -35° to -15°, from -55° to -35° and from -75° to -55° for ψ are representative, which are denoted by squared region in Fig. 6. This division of range is somewhat arbitrary but it can visualize some aspects on the structural movement with respect to time course. The unrestrained free simulation **A** accessed a more wide range of (ϕ,ψ) space(Fig. 6a), while in simulation **B** with chemical shift restraints the protein visited a more restricted range near the structured region(Fig. 6b).

The time series of the chemical shifts shown in Fig. 7 is rather self explaining. The root mean square deviation $\Delta\delta$ calculated from δ_{sec} and δ_{cal} converges to an expected tolerance value of about 0.1 ppm in simulation **B**, whilst the simulation **A** shows a random deviation around 0.5 ppm. This can also be verified in the representation of correlation plot in Fig. 8, from where rmsd $\Delta\delta$ of 0.107 and 0.453ppm and correlation coefficients $r_{cal/sec}$ of 0.970 and 0.334 for chemical shift restrained(**B**) and unrestrained(**A**) simulation can be extracted. In Fig. 8 the chemical shift values calculated from x-ray structure(1BPI) and NMR structure are also given for comparison. In the protein data bank entry of NMR

structure, pdb1pit.ent, there were 20 conformers generated using 642 distance and 115 dihedral angle constraints reported[7]. From this 20 structures we have taken 15th comformer, which revealed the 'best' correlation between measured and calculated chemical shift values. The corresponding rmsd $\Delta\delta$ were 0.531 and 0.533ppm and correlation coefficient were 0.273 and 0.126 for x-ray and NMR structure, respectively. It is surprising to note that the 'best' correlation from the 20 NMR conformers is even worse than that of x-ray solid structure, what is probably the consequence of the fact that the parameters[17] influencing the calculation of ring current and anisotropy effects were optimized[2,3] with respect to crystal structures rather than to solution structures of proteins. Therefore the correlation below 0.5 can not principally be judged by their absolute values. In all three cases besides the restrained simulation **B** there was practically no correlation between the calculated and observed chemical shift values.

Finally the experimental and calculated secondary chemical shift values with resulting rmsd $\Delta\delta$ and correlation coefficients are listed in Table 2 from simulation **A**, **B** and x-ray and NMR structure. The final MOLSCRIPT[17] pictures in Fig. 9 give an overview on the backbone structure of protein BPTI.

Table 1. Experimental and calculated chemical shift values

residue		δ_{sec}	δ_{cal}[ppm]				residue		δ_{sec}	δ_{cal}[ppm]			
			A	B	X	NMR				A	B	X	NMR
1	R	-0.06	-	-	-	-	30	C	0.93	-0.039	0.948	-0.240	-0.170
2	P	-0.11	-0.011	0.034	-0.270	-0.091	32	T	0.93	0.322	0.890	-0.396	-0.384
3	D	-0.51	-0.163	-0.542	0.070	-0.064	33	P	0.20	0.420	0.221	0.372	0.267
4	P	-0.07	0.074	0.035	0.353	0.106	34	V	-0.27	0.359	-0.352	-0.030	0.112
5	C	-0.34	0.875	-0.168	0.746	0.306	35	Y	0.28	-0.069	0.349	0.190	0.406
6	L	0.11	0.181	0.291	0.329	0.143	36	G	-	-	-	-	-
7	E	0.29	0.260	0.186	0.029	-0.054	37	G	-	-	-	-	-
8	P	0.19	0.044	0.062	-0.072	-0.084	38	C	0.26	0.091	0.124	0.104	0.119
9	P	-0.73	-0.379	-0.716	-0.480	-0.716	39	R	-0.47	0.087	-0.259	0.184	0.124
10	Y	0.33	0.543	0.405	0.191	0.111	40	A	-0.27	-0.341	-0.163	0.340	0.509
11	T	0.17	0.136	0.293	-0.169	0.135	41	K	0.08	0.043	0.056	-0.049	0.076
12	G	-	-	-	-	-	42	R	-0.75	0.229	-0.685	-0.201	-0.041
13	P	0.11	-0.146	0.173	0.027	0.035	43	N	0.29	0.434	0.146	0.400	-0.101
14	C	-0.12	0.128	-0.108	-0.024	0.075	44	N	0.14	-0.421	0.282	0.203	-0.313
15	K	0.04	0.056	0.156	0.050	-0.020	45	P	0.47	0.187	0.437	0.310	0.404
16	A	-0.05	0.022	-0.048	0.022	-0.061	46	K	0.02	-0.178	0.041	0.016	0.153
17	R	-0.09	0.186	-0.192	0.297	-0.057	47	S	0.03	0.118	0.043	0.122	-0.959
18	I	-0.04	0.027	-0.084	-0.033	-0.057	48	A	-1.21	-0.578	-1.309	-0.949	0.146
19	I	0.07	0.801	0.208	-0.410	-0.396	49	E	-0.43	-0.092	-0.245	-0.096	0.013
20	R	0.32	-0.292	0.111	-0.078	-0.043	50	D	-0.48	0.026	-0.477	-0.008	-0.018
21	Y	1.08	0.779	1.116	0.517	0.509	51	C	0.01	0.341	-0.099	-2.093	-1.556
22	P	0.60	0.349	0.435	1.321	1.040	52	M	-0.37	0.193	-0.306	0.018	0.260
23	Y	-0.31	-0.294	-0.338	0.342	0.298	53	R	-0.43	-0.031	-0.352	-0.050	-0.104
24	N	-0.15	-0.143	-0.310	-0.112	-0.353	54	T	-0.29	-0.388	-0.248	-0.039	-0.101
25	A	-0.59	0.626	-0.538	-0.119	-0.127	55	C	-0.26	0.189	-0.251	-0.404	0.043
26	K	-0.30	0.076	-0.126	-0.005	0.070	56	G	-	-	-	-	-
27	A	-0.06	0.144	0.023	0.252	0.167	57	G	-	-	-	-	-
28	G	-	-	-	-	-	58	A	-0.34	-	-	-	-
29	L	0.36	-0.055	0.379	0.224	0.039		$\Delta\delta$[ppm]		0.453	0.106	0.531	0.533
31	Q	0.46	0.147	0.285	0.074	-0.001		$r_{cal/sec}$		0.334	0.970	0.273	0.126

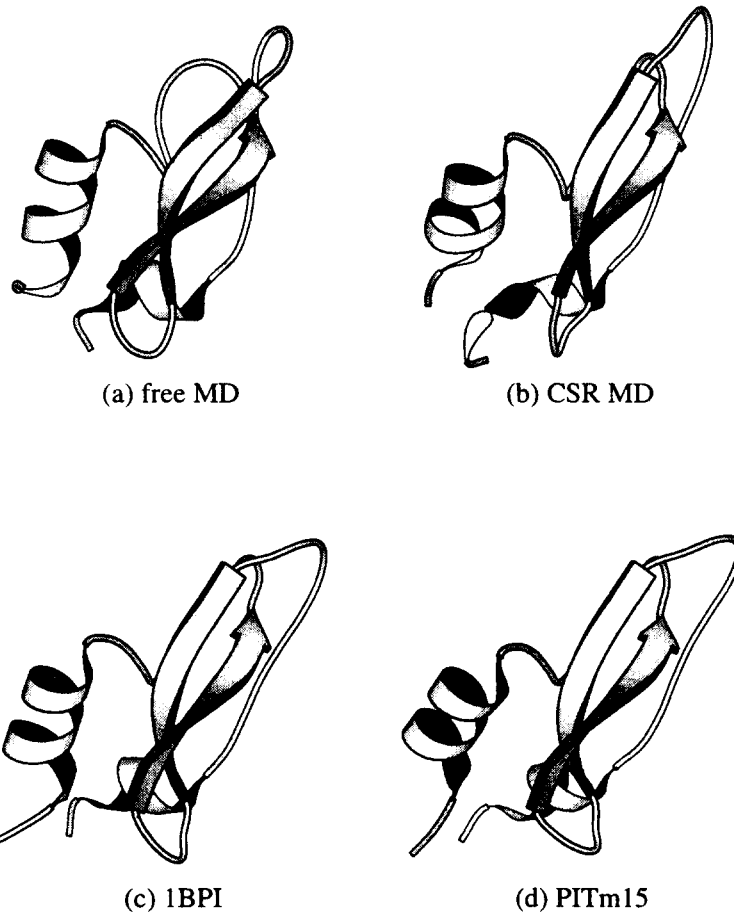

Fig. 9. Comparison of final structures from free(a), restrained(b) MD simulations, x-ray crystal(c) and NMR structure(d). The pictures were generated using the program MOLSCRIPT[18].

CONCLUSIONS

The analysis of simulated trajectories and structures described above have revealed that the primary observable of NMR experiments, chemical shift, contains very important informations about the secondary structure of protein. In conjunction with MD simulation we could deduce a reasonable solution structure

of protein BPTI, which is globally similar to the structure derived by NOE distance and dihedral angle constraints.

From the free simulation, on the other hand, we could find no inherent information in normal physical force field including only spatial electric and van der Waals interaction terms to force the protein within the structured conformation. The conformational change during this free dynamics was obviously of random character and thus the simulation length of 1.5ns is still too short to verify or disprove the possibility of another random change of conformation in a real observation time time scale.

The comparison with the NMR structure revealed definitively the potential use of chemical shift values as complementary information source. It is worth to note that 642 distance data and 115 dihedral angles were used for the deduction of 20 possible conformers[7] compatible to the input data. NMR spectroscopists often suffer from lack of sufficient distance data to reach a single unequivocal solution structure of protein. We applied in this work only 50 chemical shift values of CaH from non-Glycine residues as restraining forces to predict a reasonable solution structure of BPTI. The expense to extract and derive 757 NOE and J values from NMR measurements is clearly not comparable with that to read 50 primary chemical shift values.

The character of information from chemical shift values is also different from that of distance and dihedral angle data. Whilst the distance or J value constraint is acting on two interacting nuclei, the chemical shift restraint affects not only the position and dynamics of corresponding atom, but also the position of the members of groups contributing to the observed shift. In this sense the NOE and J derived constraints are locally restricted forces, whereas the chemical shift data can be interpreted as global forces within a more wide range of chemical shift field.

It is also interesting to note that side chains containing aromatic rings often give rise to many distance data and consequently the positions can be defined with high precision, whereas only little informations about the positions of other side chains such as Asp, Glu and Gln can be obtained. Chemical shift values contains, on the other hand, not only informations about the ring position but also the position of carbonyl containing side chains.

We, however, will mention here a couple of problems, which should be solved for the improvement of the chemical shift restraint MD methodology. Firstly, there are obviously more interaction terms contributing to chemical shift than ap-

proximated by ring current and magnetic anisotropy effects alone. For example, the inclusion of the electric field effects from nearby charged groups and axially symmetric Ca-N anisotropy effects from peptide groups would make sense. The individual value of these terms might be very small but they can be cumulative, especially if the size of the peptide chain increases and polar solvent molecules should be included explicitly into the simulation. Secondly, to get into the goal of solution structure via chemical shift restraints we need currently one starting structure, which was the crystal structure 1BPI in this work and the dependence of the final results on the starting point should also be verified in the future. We are currently investigating the inclusion of all possible contributions to chemical shifts to answer the first question. To get rid of the need of starting structure we are also planning the inclusion of all proton and ^{13}C chemical shifts. Furthermore, if one applies not only the NOE and J value constraints or chemical shift restraints separately in a competitive way but all available data simultaneously, the degree of freedom in conformation space can certainly be reduced and even better prediction of solution structure of protein can be expected.

From this results we can conclude that the chemical shift offers a very promising future in the determination of solution structure of protein. The use of chemical shift as probe for secondary structure is more complementary to the conventional distance and dihedral angle data.

Acknowledgement

This work was supported partly by Research Fellow Program(1996) of the Korea Science and Engineering Foundation.

REFERENCES

1. S. J. Perkins, and K. Wüthrich, *Biochim. Biophys. Acta,* **576,** 409 (1979).

2. M. P. Williamson, T. Asakura, E. Nakamura, and M. Demura, *J. Biomol. NMR* **2,** 83 (1992).

3. K. Ösapay, Y. Theriault, P. E. Wright, and D. A. Case, *J. Mol. Biol.* **244,** 183 (1994).

4. J. Kuszewski, A. M. Gronenborn, and G. M. Clore, *J. Magn. Reson. B* **107,** 293 (1995).

5. K. L. Park, and W. F. van Gunsteren, will be published elswhere (1997).

6. A. Wlodawer, J. Walter, R. Huber, and L. Sjölin, *J. Mol. Biol.* **180,** 301 (1984).

7. K. D. Berndt, P. Güntert, L. P. M. Orbons, and K. Wüthrich, *J. Mol. Biol.* **227,** 757 (1992).

8. A. Bundi, and K. Wüthrich, *Biopolymers* **18,** 285 (1979).

9. C. E. Johnson and F. A. Bovey, *J. Chem. Phys.* **29,** 101 (1958).

10. J. W. ApSimon, W. G. Craig, P. V. DeMarco, D. W. Mathieson, L. Saunders, *Tetrahedron* **23,** 2357 (1967).

11. W. F. van Gunsteren, S. R. Billeter, A. A. Eising, P. H. Hünenberger, P. Krüger, A. E. Mark, and W. R. P. Scott, and I. G. Tironi, *"Biomolecular Simulation: The GROMOS96 Manual and User Guide"* , BIOMOS b.v., Zürich, Groningen (1996).

12. S. Parkin, B. Rupp, and H. Hope, *Protein Data Bank of Brookhaven National Laboratory* (1995).

13. G. Wagner, W. Braun, T. F. Havel, T. Schaumann, N. Go, and K. Wüthrich, *J. Mol. Biol.* **196,** 611 (1987).

14. J. P. Ryckaert, G. Ciccotti, and H. J. C. Berendsen, *J. Comput. Phys.* **23,** 327 (1977).

15. W. F. van Gunsteren and H. J. C. Berendsen, *Angew. Chem. Int. Ed. Engl.* **29,** 992 (1990).

16. R. M. Brunne, K. D. Berndt, P. Güntert, K. Wüthrich, and W. F. van Gunsteren, *Proteins* **23,** 49 (1995).

17. K. L. Park, and W. F. van Gunsteren, *J. Kor. Magn. Reson. Soc.* **1,** (1997).

18. P. Kraulis, *J. Appl. Crystallogr.* **24,** 946 (1991).